

## Heavy mass projectile impact on thin and moderately thick unidirectional fiber/epoxy laminates

M. Ganesh Babu<sup>a</sup>, R. Velmurugan<sup>a,\*</sup> and N.K. Gupta<sup>b</sup>

<sup>a</sup>Composite Technology Centre, IIT Madras

<sup>b</sup>Department of Applied Mechanics, IIT Delhi

### Abstract

Ballistic impact tests were conducted using hard steel cylindro-conical projectiles of mass ranging between 550 to 570gms with three nose geometries against unidirectional glass-fiber reinforced epoxy composite plates of varying stacking sequence and thickness. Gas gun projectile launcher setup was used to accelerate the projectiles. The damage evolution, failure pattern, ballistic limit and energy absorption by each target set were determined experimentally. Experimental study shows that the nose geometry of heavy projectile has very less influence on the energy absorption and ballistic limit for thin targets whereas it plays a major role with increasing thickness of the laminates. It was also confirmed from the experimental study that delamination was not a major failure mechanism for thin laminates but has considerable effect on thick laminates. Severe delamination and damage were observed in thick laminates. Varying the stacking sequence neither showed marked deviation in ballistic limit nor energy absorption, but showed difference in delaminated area especially in thick targets. Results show that, while the amount of energy absorbed by the composite was different for all three projectiles, they showed similar trends - energy absorbed increased with velocity up to a critical impact velocity before it starts to decrease. A mathematical model based on energy balance principle and resistive forces acting on the projectile during perforation was developed to theoretically calculate the ballistic limit. The theoretical value correlates well with the experimental value.

Keywords: unidirectional laminates, projectiles, ballistic limit, mathematical model

## 1 Introduction

The specific stiffness and strength, tailorability to bear loads and withstand severe environments have provided engineers the incentive of using composite materials over monolithic materials for the design of many advanced structures [1]. They have been widely used in load-bearing structures as raw material cost reduces and automation of manufacturing processes increases. The increased use of composite materials, particularly in the transport industry, e.g. in the design of aircraft, helicopters, boats, cars, etc. requires a detailed understanding of the behavior of

---

\*Corresp. author email: rvel@iitm.ac.in

Received 14 Nov 2006; In revised form 16 Apr 2007

the composite component or structure to a wide range of potential external loadings, some of which may be severe [3]. The sheet applications of the composite materials cause increasing concern because they are susceptible to impact damage, which can lead to significant reduction in strength. Particularly in the aerospace industry, impact damage in laminated composite materials continues to be a major cause of concern. Therefore, understanding impact response and subsequent damage mechanisms, and assessing residual strengths are essential for the successful use of these materials. There are many practical situations where plate structures are subjected to transient impact loading of high intensity. Transient deformations are induced ranging from small-deflection linear elastic behaviour to large-deflection elasto-plastic behaviour with permanent deformation. Local damage and even failure of plates may take place. In such cases, it is essential to perform impact analysis for the purpose of plate design and/or verification. Structural intensity occurs as a result of dynamic impact loading.

The damage mechanisms is very complex, unlike metals, and depend on many parameters such as impact velocity, impact angle, nose shape of the projectile, target material, target geometry and boundary condition. The impact properties of laminated composites are influenced significantly by the fiber orientation angle, lamination configuration and specimen geometry [8].

Impact on target has been classified into two major categories based on the velocity of the moving projectile [2]. During high-velocity impact, the target response is controlled by local behavior of the material because of relatively small impact mass and short contact duration so that available kinetic energy is likely dissipated over a small zone surrounding the contact area. The failure mode is dominated by perforation. Low-velocity impact is usually associated with relatively large impact mass and long contact duration so that the entire target structure responds, thereby enabling more kinetic energy to be absorbed elastically. Under such conditions, the dynamic response is important, and damage is strongly affected by the target geometry and material properties [12]. Typical failure modes are matrix cracking, surface micro buckling, delamination, fibre shear-out and fibre fracture. In particular, delamination is a major damage mode due to the relatively low interlaminar shear strength of composite materials.

Chambers et al [4] studied the damage in unidirectional carbon/fibre composite resulting from both low and high velocity/energy impacts using embedded fibre Bragg grating (FBG) sensors, C-scan and microscopic analysis. They showed that the FBG sensors located 10 mm from the impact site detected residual strains from a 0.33 J impact but was not detected by C-scan or visual inspection. The measured residual strain increased with impact energy and damage changed from matrix cracking to severe delamination. High velocity impacts resulted in test panel perforation and delamination.

Moura and Marques [5] has performed numerical and experimental analyses for predicting the damage in two carbon-epoxy laminates subjected to low velocity impact. Damage characterization was carried out using X-ray radiography and the deply technique. Good agreement between the experimental and numerical analysis for shape and orientation of delamination was obtained.

Lim et al [6] carried out experiments to investigate the impact phenomenon of double-ply

systems that consisted of Twarons CT 716 fabric and projectiles of hemispherical, flat, ogival and conical nose. Results obtained revealed that the increase in energy absorption was not doubled when the ply number was increased to two. The ratio of energy absorbed in the double-ply system to that of the single-ply system varied with impact velocity and projectile geometry. Failure mechanisms of a double-ply system were similar to that of a single-ply system, but the degree of damage of the impact and distal plies differed.

Will, Franz and Nurick [11] focused on the effect of change in the laminate stacking sequence on the ability to dissipate kinetic projectile energy. Two different T800 carbon fibre filament wound tubes in an epoxy matrix with two lay-up sequence were investigated. The tubes were subjected to impact up to and above the ballistic limits. The energy dissipated by material failure and friction was quantified and shown to be similar for the two laminates at the respective ballistic limits.

In our earlier work [9], energy absorption and ballistic limit of different composite system were studied and a mathematical based on energy balance principle was developed. The damage pattern was also analyzed. Of all the tested laminates WRM/epoxy showed the highest ballistic limit. The model also showed good agreement with the experimental value.

The behavior of different E-glass/epoxy laminated composite plates has been experimentally studied under impact of aluminum projectile at low velocities by Mili and Necib [7]. The results were obtained using a drop weight impact machine and presented for three different cross-ply laminates. The time history of the impact process was measured. The effects of the projectile velocities and lamination sequences on composite plate's behavior have been discussed.

In the present work the impact behavior of unidirectional glass epoxy laminated composites have been studied as a function of fiber orientation angle, lamination configuration and projectile nose geometry. The energy absorbed by each type of target and the corresponding ballistic limit were determined experimentally. A mathematical model was developed to theoretically predict the ballistic limit.

## 2 Experimental

### 2.1 Specimen preparation

Targets were constructed from unidirectional E glass with 4 and 6 plies of a nominal 600 gm-s unidirectional mat and commercially available Epoxy resin (LY556). The laminates were hand layed on a flat aluminium mould and cured with 10% by mass of TETA hardener (HY 951) at room temperature for a day and finally post cured for 3 hrs at 80°C. Two stacking sequences were employed for 6 layered laminate viz (0,45,90)2s, (0,45,90,90,-45,0), and (0,90)2s for 4 layered laminates. The 6 layered laminate had 2 thickness ranges due to difference in the aerial density of the UD mat, but with similar stacking sequence and ply count. A fiber mass fraction of 0.5 was maintained for all the laminates. After complete curing, the panels were cut into 290 x 290 mm square specimens by band saw. Thickness measurements were taken at eight points on

each specimen prior to testing. Sample specimens for quasi-static tests were cut from the same laminate. Material properties of each set of laminate were shown in Table 1.

Table 1: Material properties of different laminates

Material Properties	4 Layers	6 Layers Symmetric	6 Layers Symmetric	6 Layers Anti Symmetric	6 Layers Anti Symmetric
Youngs Modulus (E) GPa	31	32	32	31	31.5
Average panel thickness (mm)	2.3	3.2	4.9	3.2	4.9
Tensile Strength (MPa)	180	186	202	183	204
Flexural Strength (Mpa)	260	340	211	350	221
Interlaminar shear strength (MPa)	17	28	26	28	26
Impact strength (J/cm)	15	17	22	18	24

## 2.2 Quasi-static test

Quasi-static tests were performed on the samples that were cut from the panels. Tensile, flexural and interlaminar shear strengths were determined using a Universal Testing Machine. ASTM standards were adopted for carrying out the quasi static tests. Izod impact test was performed on the sample using Izod impact testing machine as per ASTM D 256. Samples of 5 were tested for each test. Table 1 shows the material properties of the unidirectional laminates.

## 2.3 Impact test

A piston type gas gun setup was employed to perforate the targets at various speeds. The experimental set up shown in Figure 1 is explained in our earlier paper [9]. Three types of cylindro-conical projectiles with different nose geometries were used to perforate the targets. Figure 2 shows the photograph of the projectiles and their nose geometry and Table 2 shows the projectile characteristics. From the experiment the ballistic limit and energy absorption by the target for various projectile geometry and speed were deduced.

The ballistic limit was taken to be the average of two striking velocities, one being the highest velocity giving a partial penetration and the other lowest velocity giving a complete penetration.

## 2.4 Analytical model

An analytical model was developed to predict the ballistic limit of different target material subjected to projectile impact. The initial kinetic energy possessed by a moving projectile was either completely absorbed or partially absorbed by the target during perforation. The former occurs before reaching the ballistic limit and the later, after achieving the ballistic limit. The



Figure 1: Gas Gun projectile launcher – Experimental setup



Figure 2: Cylindro-conical projectiles with three different nose geometries

Table 2: Projectile Characteristics.

Projectile characteristics	Cylindro conical projectile		
	Sharp nose	Rounded nose	Truncated nose
Length of the Projectile ( $L_p$ )	100	100	100
Shank Length ( $L_s$ )	56	56	56
Nose Length ( $L_n$ )	44	44	44
Projectile Radius ( $R_p$ )	19.6	19.6	19.6
Mass (M)	556.8	560	561
Cone Angle ( $\theta$ )	$60^\circ$	45	45

energy absorbed by a target when subjected to projectile impact can be divided into three stages.

- **Stage I** Energy absorbed due to elastic deflection of the target.
- **Stage II** Energy absorbed by the target during the entry of the nose portion of the projectile.
- **Stage III** Energy absorbed during the entry of the projectile's shank portion.

**Stage I** – the stage where no perforation occurs but work being spent in deflecting the target. The force exerted at tip of the projectile will force the target to undergo deflection. It was already observed that the response of target during low velocity impact is structural dominant and is not localized. Similarly, impact by heavy projectile on moderately thick target is also global. Hence more energy is absorbed elastically. A portion of the kinetic energy possessed by the projectile will be spent on bending the target. Beyond the maximum deflection, the target will fail and facilitates the entry of the projectile. A quasi static punch test data showed that the force applied to the target by the projectile before perforation is almost half of the total force required to achieve complete perforation, suggesting that the bending of the target material will absorb a major portion of the projectiles initial kinetic energy.

The energy absorbed in the elastic region due to the bending of plate is given by

$$E_e = \frac{3\pi r^2 t (1 - \nu^2) \sigma_y^2}{8E} \quad (1)$$

**Stage II** – Penetration stage. The target after reaching the maximum deflection, undergo failure due the force exerted by the moving projectile. The energy required to overcome the resistive force offered by the target medium was calculated from the model proposed by Wen [10]. According to H.M.Wen, the mean pressure ' $\sigma$ ' applied normally to the surface of the projectile by an FRP laminate material to resist penetration and perforation is divided into two parts.

One is the cohesive quasi static resistive pressure ' $\sigma_s$ ' due to elastic-plastic deformations of the laminate material and the other is the dynamic resistive pressure ' $\sigma_d$ ' due to velocity effects. Hence the mean resistive pressure is given by

$$\sigma = \sigma_s + \sigma_d \quad (2)$$

It was also assumed that the quasi-static resistive pressure is equal to the quasi-static linear elastic limit ' $\sigma_e$ ', since the elastic deformation occurs within this limit.

$$\sigma_s = \sigma_e \quad (3)$$

This elastic limit was already considered in the first stage and hence the term  $\sigma_s$  is omitted and only the dynamic resistive pressure is considered.

The dynamic resistive is a function of the parameter 'D' and is taken to be

$$\sigma_d = D\sigma_e = \sigma \quad (4)$$

Where

$$D = \beta \sqrt{\frac{\rho_t}{\sigma_e}} \cdot Vi. \quad (5)$$

where  $\beta$  is a function of nose geometry and is equal to

$$\beta = 2 \cdot \sin \theta / 2 \quad (6)$$

$$\sigma = \beta \sqrt{\frac{\rho_t}{\sigma_e}} \cdot Vi \cdot \sigma_e \quad (7)$$

The resistive force 'F' of a projectile penetrating a target medium at normal incidence is given by

$$F = \sigma A \quad (8)$$

Where 'A' is the cross sectional area of the projectile, given by

$$A = \pi r^2 \quad (9)$$

Hence resistive force 'F' becomes

$$F = \pi r^2 \sigma_y \beta \sqrt{\frac{\rho_t}{\sigma_e}} \cdot Vi \quad (10)$$

From energy conservation,

$$E = \int_0^t F \cdot dT \quad (11)$$

$$E = \pi r^2 t \beta \sqrt{\rho_t \sigma_e} V_i \quad (12)$$

**Stage III** – In the third stage only the friction between the target and the projectile exist and no other resistive force act on the projectile. It was assumed that there exist a constant friction between the two and the energy absorbed is given by

$$E_{fric} = F_f \cdot L_p \quad (13)$$

where ‘F’ is the frictional force. The coefficient of friction is taken to be constant and is equal to 0.35.

## 2.5 Energy absorbed due to plugging

Plugging occurs only in the case of flat projectile and projectile with truncated nose. A band of high shear strain is produced at a radius close to the projectile radius and this result in a plug being sheared off. This shear band is a special case for flat projectile and cannot be seen in other types. The energy required to eject a plug of radius equal to the radius of the projectile is given by

$$E = 2\pi r t \tau x \quad (14)$$

Combining the energy terms, substituting  $E = (1/2)MV^2$ , and rearranging the terms yields the ballistic limit for each projectile.

Total energy absorbed is

$$\frac{MV_i^2}{2} = \frac{3\pi r^2 t (1 - \nu^2) \sigma_y^2}{8E} + \pi r^2 t \beta \sqrt{\rho_t \sigma_y} V_i + F_f \cdot L_p \quad (15)$$

For truncated nose projectile an additional plugging energy term is included and hence equation (15) becomes

$$\frac{MV_i^2}{2} = \frac{3\pi r^2 t (1 - \nu^2) \sigma_y^2}{8E} + \pi r^2 t \beta \sqrt{\rho_t \sigma_y} V_i + F_f \cdot L_p + 2\pi r t \tau x \quad (16)$$

After solving the above equation, the expression for ballistic limit is given as

$$V_b = \frac{\pi r^2 t \beta \sqrt{\rho_t \sigma_y} \left( 1 + \left[ \sqrt{1 + \frac{2MC^2}{(\pi r^2 t \beta \sqrt{\rho_t \sigma_y})^2}} \right] \right)}{M} \quad (17)$$

Where ‘C’ is given by

$$C = \frac{3\pi r^2 t (1 - \nu^2) \sigma_y^2}{8E} + F_f \cdot L_p + 2\pi r t \tau x \quad (18)$$

### 3 Results and discussion

#### 3.1 Damage evolution and failure pattern:

All the targets are subjected to different projectile impact up to and above the ballistic limit. The damage area observed on the front side was almost equal to the diameter of the projectile, whereas, the exit side shows an increased damage area for all types of projectiles. Separation of bottom most ply from the laminate starting from the point of impact and along the entire length on either side was observed for almost all laminates on the exit side, as shown in the Figure 2. Only two sides of the target are clamped and when this is subjected to impact load a cylindrical bending occurs rather dishing which is predominant in the case of targets clamped on all the four sides. Due to this bending, the transverse fibers holding the longitudinal fibers fail first and allow the crack to propagate across these fibers easily. Hence the bottommost ply tends to get separated from the laminate. In the case of thicker laminates, such separation was not observed instead, fibers in the damage area gets separated individually as seen in Figure 3. It is also observed that the extent of this delamination is almost equal to the diameter of the damage area. When the laminate is clamped in the other direction this type of failure was not observed since the clamping force offered by the clamps holds all the layers together (Figure 4). With increase in plate thickness and impact velocity, the local effect becomes more important and the effect of structural response on the target perforation reduces. Increase of plate thickness, impact velocity and bluntness of the projectile, shear plugging becomes a likely failure mode of the final perforation of the target. It can be observed from the figure that damage in the form of plugging has occurred when the target is struck by truncated projectile. This was not observed in the case of sharp and blunt projectiles. Figure 5 shows the cross sectional view of damaged area of laminates subjected to impact by different nose geometry. It can be seen from the figure that, all the fibers under the point of impact has undergone failure. Extensive damage and delamination was observed on the last ply and failure in all the layers.

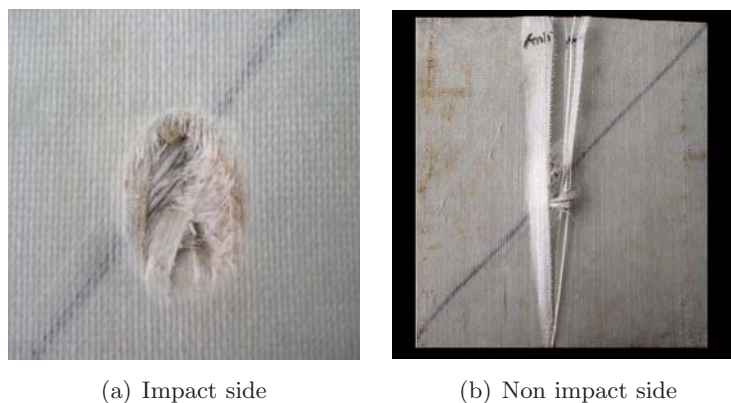


Figure 3: Damage area on the 6 layered symmetric target struck by sharp projectile.

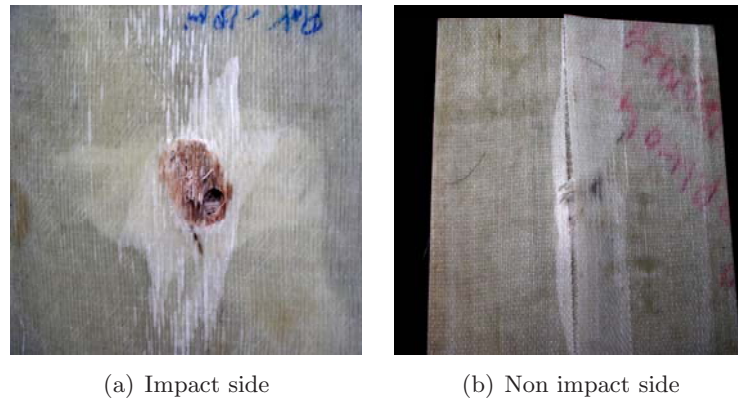


Figure 4: Damage area on the 6 layered symmetric target struck by truncated nose projectile.



Figure 5: Damage area observed on the impact side and on the non impact side for a 6 layered Anti symmetric thick laminate.

### Delamination

During the entry of the projectile into the target, the material gets displaced laterally as well as downwards, producing a localized deformation around the impact region and global deflection away from the point of impact resulting in in-plane compression. This results in interlaminar cracking of Mode I and Mode II type combined together. The impact produces mode I delamination which is extended by the penetration of the projectile. The first possible failure that occurs in a target when subjected to impact is matrix cracking. Matrix cracking leads to decrease in the interlaminar strength of the composite, as a result, further loading and deformation causes delamination. Varying the angle between two layers affects the extent of delaminated area when subjected to impact. Maximum delaminated area is observed for laminates with an orientation angle between two adjacent layers being  $90^\circ$ . The delaminated area on the impact side is different from the non-impact side. Impact side shows less delamination whereas non-

impact side shows more delaminated area (Figure 6). It has been reported [13] earlier that, the delamination, either in static or dynamic case does not dissipate a major amount of energy. For thin laminated composite panels excessive delamination is not observed. It was noted from the experiment that with an increase in thickness and bluntness of the projectile, the delamination area between the layers becomes more and complex. Thin laminates showed regular damage pattern with less delaminated area for all types of projectile impact except for the separation of the bottommost ply from the rest of the laminate as seen from figure. Thicker laminates also shows an increased delaminated area. As the thickness of the target increases the bending resistance offered by the target increases due to increase in stiffness. For thick laminates, the severe delamination was observed when struck by truncated projectile and the delamination was mainly observed along the primary yarns.



Figure 6: Damage area observed on the impact side and on the non impact side for a 4 layered laminate clamped in the opposite direction.

The delaminated area for laminates struck by the projectiles with different nose geometry is slightly above the damage area as seen in Figure 6. All the tested specimens show a difference in delaminated area for front and back side of the target. It was also concluded from the experimental observation that by varying the orientation angle there is no significant effect on the delaminated area.

### Friction

Penetration occurs once the fibers under the point of impact fail due to tension. The failure of the yarn provides a path for the projectile to enter into the target. The projectile has to overcome frictional resistance provided by the damaged laminate. The friction decreases with increasing sliding velocity between the projectile and the plate target. It is also reported that the friction between the target and the projectile increases up to the nose length and then remains constant until the projectile emerges out of the target. The variation in friction along the nose length depends on the cone angle. For cylindro-conical projectile with sharp nose, the variation in friction along the nose length is more when compared to the friction for truncated or

blunt nose. This is noticed typically for heavy projectiles moving with a moderate velocity. The friction in the nose portion increases till the nose enters the target and then remains constant for the rest of the shank length. With an increase in the cone angle, the frictional resistance also increases. The friction in the shank portion remains constant for all the projectiles of similar diameter.

#### Failure of fibers

During the ballistic impact event the energy of the projectile is transferred to the target. The energy is absorbed by the deformation of the secondary yarns, failure of the primary yarns, delamination and matrix cracking. Failure of primary yarns and secondary absorbs more energy next to energy absorbed due to bending of target.

Figure 7 shows the SEM picture of a UD laminate subjected to tensile failure. Failure has occurred only in the middle layers which are  $90^\circ$  in nature and these are the only layers that are parallel to the loading direction. The other layers which are  $0^\circ$  and  $45^\circ$  in nature do not take part in bearing the load. But during a ballistic event, all the fibers directly under the point of impact will take up the force exerted by the projectile and all the layers will fail. Figure 8 shows the failure of fibers in all the layers indicating that orientation of fiber does not play a major role in a ballistic event. From the Figure 9 it can be seen that bottom most ply due to bending undergoes more delamination than other layers.

### 3.2 Ballistic limit

The ballistic limits of the laminates with different fiber orientation and varying target thickness as a function of nose geometry were determined experimentally. It is a statistical measure of the velocity at which penetration just occurs. Ballistic limit or the limiting velocity is the indication of projectile's minimal initial velocity which is sufficient enough to cause perforation in the target. All the laminates were subjected to impact at various projectile velocities. The minimum velocity required to achieve the ballistic limit for each projectile was determined experimentally. The residual velocity possessed by the projectile after penetration was also recorded. The energy absorbed by different targets for various initial velocities of the projectile is determined from the residual energy possessed by the projectile after penetration and plotted as a function of projectile initial velocity. From the experimental investigation it is observed that the projectile with truncated nose requires high velocity to perforate the target material and thus recording the highest ballistic limit. The initial area available to cause perforation in the target is more for truncated nose projectile; more energy is required to fail the target material and hence shows an increase in the ballistic limit. Sharp nosed projectile with a cone angle of  $45^\circ$ , which is less than that of other two types, requires least energy to perforate the target and thus a representative of projectile possessing lowest ballistic limit. The ballistic limit for the projectile with blunt nose lies between these. The initial area available to penetrate the target medium is higher for blunt nose when compared to area available for sharp nose but less than that of flat nose and hence



(a) 4 layered laminate



(b) 6 layered symmetric laminate



(c) 6 layered symmetric thick laminate



(d) 6 layered symmetric thick laminate

Figure 7: Cross sectional view of different laminate showing damage pattern subjected to sharp nose projectile impact.

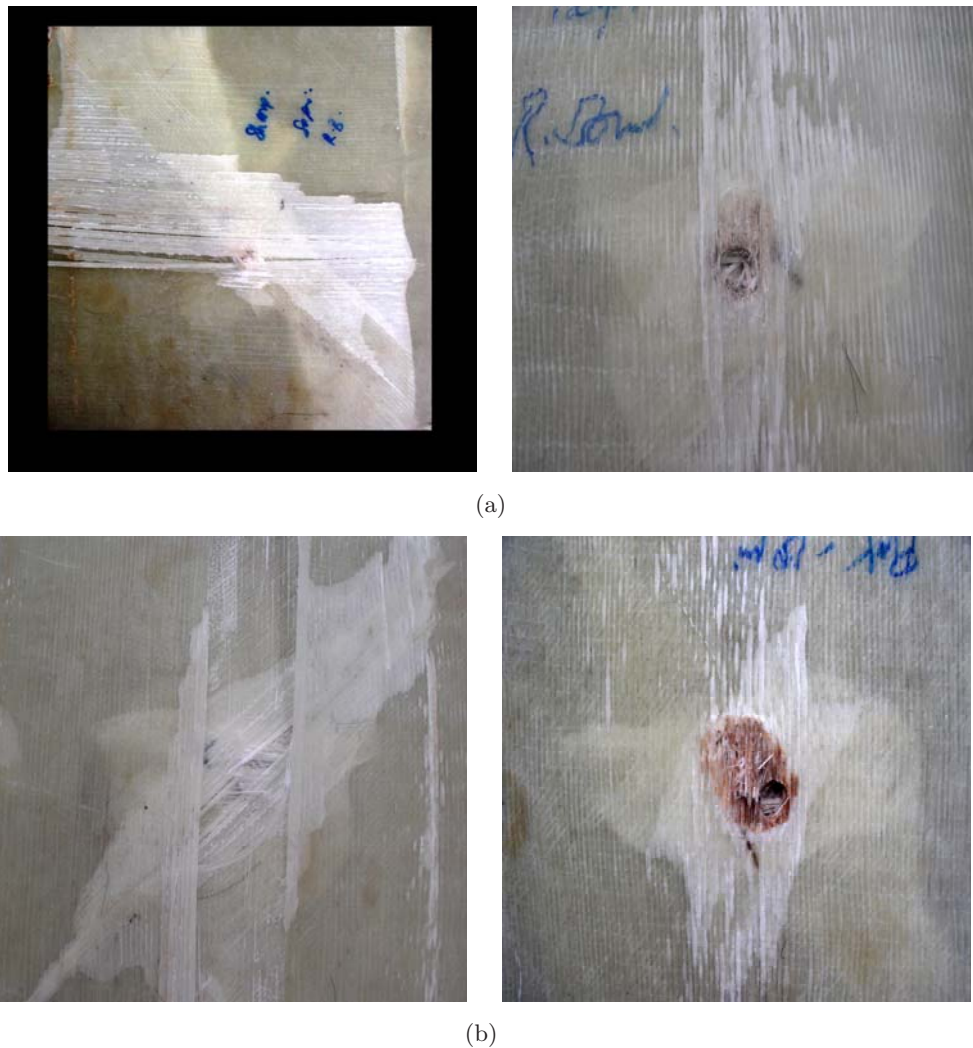


Figure 8: Thick laminates showing extensive delamination struck by (a) Blunt projectile front and back side (b) Truncated nose projectile, front and back.

the limiting velocity lies between flat and sharp nosed projectile. Similar trend is observed for both symmetric and anti-symmetric laminates. But symmetric laminates showed slightly higher ballistic limit when compared to its counterpart. It was also observed that the energy absorption increases with increase in thickness and shows similar trend in the ballistic limit as well. A marked deviation in ballistic limit was observed for thick laminates struck by different projectile but it is not the case of thinner ones. The deviation in ballistic limit with change in nose shape is not well established for such thin laminates. This indicates that change in nose shape for a heavy mass cylindro-conical projectile does not have much influence in ballistic limit

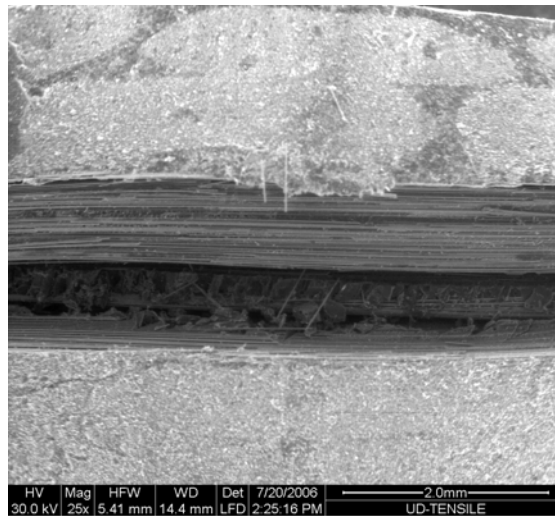


Figure 9: SEM picture of (0,45,90)s specimen subjected to tensile load showing failure in the middle layers.

for thinner laminates. But a significant change in ballistic limit was observed for thick targets.

Figure 10 shows the final velocity of the projectile with different nose geometry as a function of initial speed. The residual velocity remains zero up to a certain value of the initial velocity and then increases with the initial velocity. Beyond the ballistic limit, complete penetration occurs and the projectile emerging out of the target possesses residual kinetic energy. Figure 11 shows the damage at ballistic limit for sharp and blunt projectile. At velocities below ballistic limit the perforation of the target does not take place but shows damage

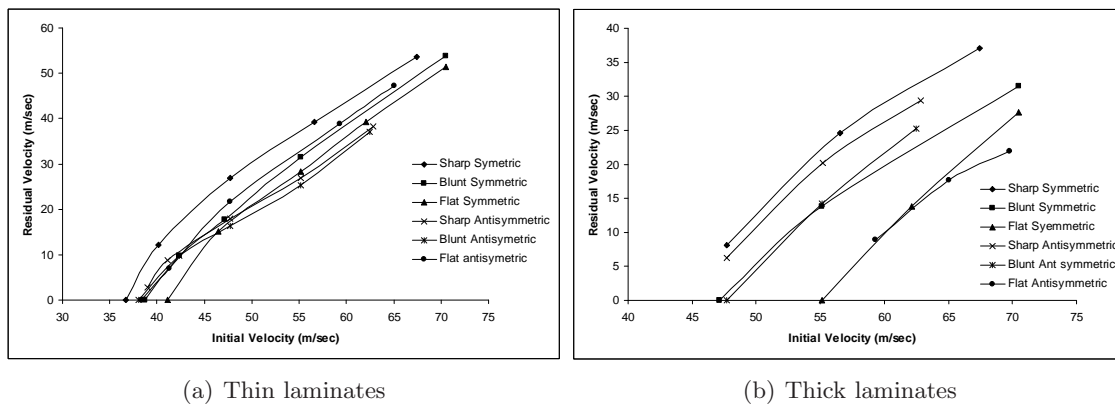


Figure 10: Variation of residual velocity with initial velocity for 6 layered thin and thick laminates subjected to impact using projectiles of varying nose geometries.

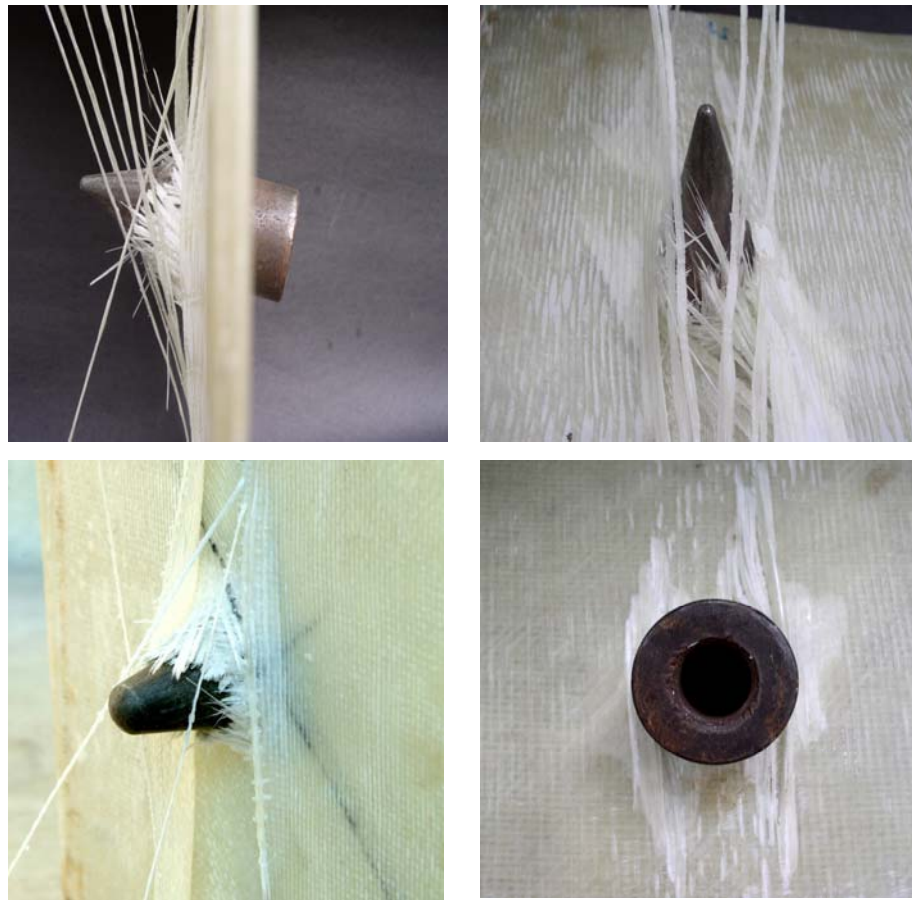


Figure 11: Damage in laminates at ballistic limit. (a) Sharp nose (b) Blunt nose.

Table 3: Ballistic limit of laminates for different nose geometry

Projectile Nose Geometry	Ballistic limit (m/sec)				
	4 layers (0,90)	6 Layers symmetric	6 Layers symmetric	6 Layers - anti symmetric	6 Layers - anti symmetric
Sharp nose	30	37	37	45	46
Blunt nose	32	40	39	50	49
Truncated nose	36	46	45	58	58

### 3.3 Energy absorption

Variation in energy absorption by targets subjected to impact by different projectile is shown in Figures 12 and 13. An increase in energy absorption with increase in the initial energy of the projectile is observed for all the case. At impact velocities below the ballistic limit, the energy absorbed equals the impact energy and is therefore identical for all projectiles and target set. The incident energy is absorbed completely by the target before reaching the ballistic limit. After reaching the ballistic limit, there is still an increase in energy absorption. The energy absorbed by the different projectile starts to deviate from one another once the ballistic limit is exceeded. At high initial velocity, there is only slight increase in energy absorption. At velocities above the ballistic limit, the contact time between the target and projectile is more and so the energy is absorbed by all the energy absorbing mechanisms. But for high initial velocities, the response time for the target is less and the impact event becomes more localized resulting in decreased energy absorption. The residual velocity also increases with increase in the initial velocity at high velocity regime because of the reduced friction. From the figure, the maximum energy absorbed during impact process corresponds to the target that is struck by truncated tip projectile. For sharp and round projectiles, the initial contact between the target and the projectile is a point contact and hence the entire load will be concentrated at the point of impact, but for truncated nose, the load will be distributed across the flat portion of the tip and hence requires more energy to initiate the perforation.

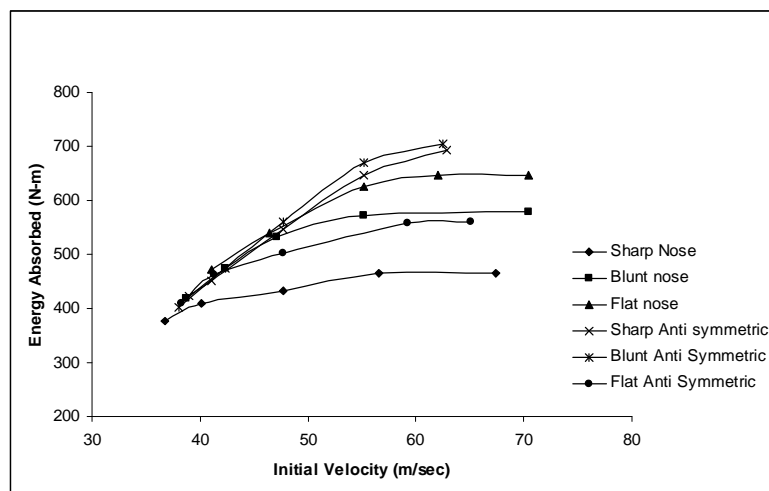


Figure 12: Variation of energy absorption as a function of initial velocity for 6 Layered thin laminates.

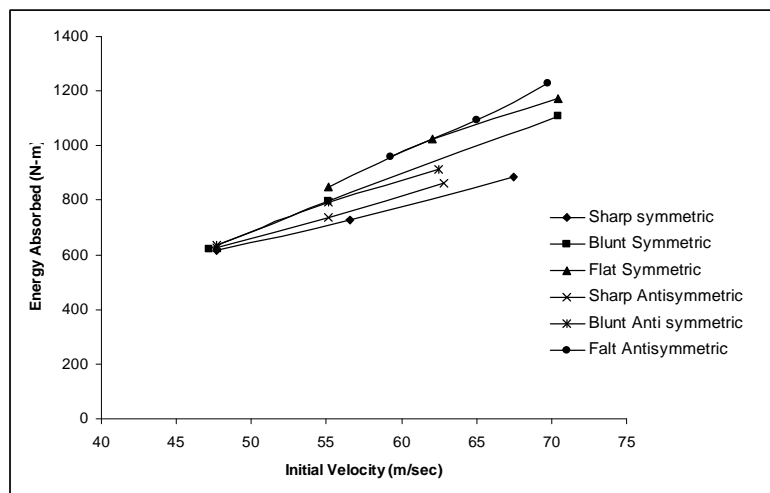


Figure 13: Variation of energy absorption as a function of initial velocity for 6 Layered Thick laminates.

#### 4 Conclusion

An experimental investigation of the penetration of unidirectional laminate by projectiles of different geometries has been conducted for various impact velocities. Cylindro-conical projectile with truncated nose geometry impact resulted in greatest amount of energy absorption at ballistic limit followed by blunt and sharp nose projectiles. Panel thickness has a significant effect on the ballistic limit of panels impacted by projectiles with different nose geometry. Perforating a comparatively thin target by heavy projectile of different geometry does not show marked deviation in the ballistic limit and energy absorption. Experimental investigation also shows that the variation in projectile geometry does not significantly affect the damage and delaminated area for thin panels. Plugging has occurred in thick targets struck by truncated nose projectile.

#### References

- [1] S. Abrate. Impact on laminated composite materials. *Applied Mech Review*, 44(4):155–90, 1991.
- [2] C.E. Anderson Jr. and S.R. Bodner. Ballistic impact: the status of analytical and numerical modelling. *Int Journal of Impact Engineering*, 7:9–35, 1988.
- [3] M.E. Backman and W. Goldsmith. The mechanics of penetration of projectiles into targets. *Int J of Engineering Science*, 16:1–99, 1978.
- [4] A.R. Chambers, M.C. Mowlem, and L. Dokos. Evaluating impact damage in cfrp using fibre optic sensors. *Composites Science and Technology*, 2006. available online.

- 
- [5] M.F.S.F. de Moura and A.T. Marques. Prediction of low velocity impact damage in carbon-epoxy laminates. *Composites Part A – Applied Science and Manufacturing*, 33(3):361–368, 2002.
- [6] C.T. Lim, V.B.C. Tan, and C.H. Cheong. Perforation of high-strength double-ply fabric system by varying shaped projectiles. *International Journal of Impact Engineering*, 27:577–591, 2002.
- [7] F. Mili and B. Necib. Impact behavior of cross-ply laminated composite plates under low velocities. *Composite Structures*, 51:237–244, 2001.
- [8] V.B.C. Tan, C.T. Lim, and C.H. Cheong. Perforation of high-strength fabric by projectiles of different geometry. *International Journal of Impact Engineering*, 28:207–222, 2003.
- [9] R. Velmurugan, N.K. Gupta, and Ganesh Babu. Energy absorption and ballistic limit of targets struck by heavy projectile. *Latin American Journal of Solids and Structures*, 2005. Available online.
- [10] H.M. Wen. Predicting the penetration and perforation of frp laminates struck normally by projectiles with different nose shapes. *Composite Structures*, 49:321–329, 2000.
- [11] M.A. Will, T. Franz, and G.N. Nurick. The effect of laminate stacking sequence of cfrp filament wound tubes subjected to projectile impact. *Composite Structures*, 58:259–270, 2002.
- [12] E. Zaretsky, G. deBotton, and M. Perl. The response of a glass fibers reinforced epoxy composite to an impact loading. *International Journal of Solids and Structures*, 41:569–584, 2004.
- [13] G. Zhu., E. Goldsmith, and C.K.H. Dharan. Penetration of laminated kevlar by projectiles – II analytical model. *International Journal of solids and structures*, 29(4):421–436, 1992.

